Nosé–Hoover chains: The canonical ensemble via continuous dynamics

Glenn J. Martyna and Michael L. Klein
Department of Chemistry, University of Pennsylvania, Philadelphia, Pennsylvania 19104-6323

Mark Tuckerman[a)]
Department of Chemistry, Columbia University, New York, New York 10027

(Received 8 April 1992; accepted 4 May 1992)

Nosé has derived a set of dynamical equations that can be shown to give canonically distributed positions and momenta provided the phase space average can be taken into the trajectory average, i.e., the system is ergodic [S. Nosé, J. Chem. Phys. **81**, 511 (1984), W. G. Hoover, Phys. Rev. A **31**, 1695 (1985)]. Unfortunately, the Nosé–Hoover dynamics is not ergodic for small or stiff systems. Here a modification of the dynamics is proposed which includes not a single thermostat variable but a chain of variables, Nosé–Hoover chains. The "new" dynamics gives the canonical distribution where the simple formalism fails. In addition, the new method is easier to use than an extension [D. Kusnezov, A. Bulgac, and W. Bauer, Ann. Phys. **204**, 155 (1990)] which also gives the canonical distribution for stiff cases.

I. INTRODUCTION

Temperature control in molecular dynamics simulations (Newtonian dynamics) is essential as most experimental measurements are performed at constant temperature rather than constant energy. Nosé resolved this difficulty by deriving a dynamics from an extended Hamiltonian that can be shown to give canonically distributed positions and momenta.[1–4] The proof, however, involves the assumption that the dynamics itself is ergodic or, more succinctly, that the trajectory average can be taken into the phase space average. It has since been shown that for small or stiff systems the dynamics is not ergodic and the correct distributions are not generated.[2,5] The method does, however, work extremely well in large (ergodic) systems.

In this article, a possible reason for the nonergodicity of Nosé's original formulation is discussed. A simple modification based on this analysis is presented and tested on model problems. The method proposed herein succeeds precisely where the original method fails. The present modification has the advantage that it preserves the simplicity of the original approach.

Other methods can also be used to obtain canonical distributions on stiff systems,[6–9] some of which are variations and generalizations of the original Nosé–Hoover approach.[7–9] In the general method of Kusnezov *et al.*, the choice of functions and parameters is somewhat arbitrary and the algorithm difficult to apply in complex situations such as constant pressure simulations. The method of Andersen which involves stochastic collisions (at intervals some or all of the velocities are resampled according to the Boltzman distribution) will also give the canonical ensemble even in the most trivial systems.[6] This method has the disadvantage that it is not a continuous dynamics with well defined conserved quantities. Hence the same trajectory cannot easily be reproduced by another worker from the same initial conditions. The present scheme preserves the advantages of the original Nosé–Hoover approach.

II. METHODS

The set of dynamical equations,[1–4]

$$\begin{aligned}\dot{q}_i &= \frac{p_i}{m_i},\\ \dot{p}_i &= -\frac{\partial V(\mathbf{q})}{\partial q_i} - p_i\frac{p_\eta}{Q},\\ \dot{p}_\eta &= \sum_{i=1}^{N}\frac{p_i^2}{m_i} - NkT,\\ \dot{\eta} &= \frac{p_\eta}{Q},\end{aligned} \tag{1}$$

defines Nosé–Hoover dynamics. Here p_i and q_i are one dimensional variables and the variable η, which is decoupled from the dynamics, is included for completeness. This set of equations, can be shown to give the canonical distribution in an ergodic system.[1,2] A proof due to Hoover uses conservation of probability[2] to show that the distribution

$$f(\mathbf{p},\mathbf{q},p_\eta,\eta) \propto \exp\left[-\frac{1}{kT}\left(V(\mathbf{q}) + \sum_{i=1}^{N}\frac{p_i^2}{2m_i} + \frac{p_\eta^2}{2Q}\right)\right] \tag{2}$$

is stationary

$$\frac{\partial f}{\partial t} + \sum_{i=1}^{N}\frac{\partial f}{\partial q_i}\dot{q}_i + \frac{\partial f}{\partial p_i}\dot{p}_i + \frac{\partial f}{\partial p_\eta}\dot{p}_\eta + \frac{\partial f}{\partial \eta}\dot{\eta} + f\left[\frac{\partial \dot{q}_i}{\partial q_i} + \frac{\partial \dot{p}_i}{\partial p_i} + \frac{\partial \dot{\eta}}{\partial \eta} + \frac{\partial \dot{p}_\eta}{\partial p_\eta}\right] = 0. \tag{3}$$

Therefore (if the system is ergodic), $f(\mathbf{p},\mathbf{q},p_\eta,\eta)$ is the static probability distribution generated by the dynamics. The proof is necessary but not sufficient for a general system.[2–4,10] In addition, it can be shown that the quantity

[a)]In partial fulfillment of the Ph.D. in the Department of Physics, Columbia University.

 0021-9606/92/162635-09$006.00

$$H'(\mathbf{p},\mathbf{q},\eta,\mathbf{p}_\eta)=V(\mathbf{q})+\sum_{i=1}^{N}\frac{p_i^2}{2m_i}+\frac{p_\eta^2}{2Q}+NkT\eta \qquad (4)$$

is conserved, namely,

$$\frac{dH'}{dt}=\sum_{i=1}^{N}\frac{\partial H'}{\partial p_i}\dot{p}_i+\frac{\partial H'}{\partial q_i}\dot{q}_i+\frac{\partial H'}{\partial p_\eta}\dot{p}_\eta+\frac{\partial H'}{\partial \eta}\dot{\eta}=0. \qquad (5)$$

This is why it is useful to include the variable η in Eq. (1). In Appendix A, the extension due to Kusnezov *et al.* and the method of Winkler are discussed.[3,7,9]

The proof presented above is valid only for ergodic systems. It does not guarantee that the system is ergodic and that the correct limiting distribution will be generated. Indeed, in some cases, this distribution is not produced.[2–4] Let us consider how this situation can be improved. The distribution itself has a Gaussian dependence on the particle momenta, p, as well as thermostat momenta, p_η. While the Gaussian fluctuations of p are driven with a thermostat, there is nothing to drive the fluctuations of p_η. Although the postions and momenta (the q's and p's) are of primary interest, if the Nosé–Hoover equations are ergodic, the system covers the whole phase space, which includes the space of the thermostat velocities. The fluctuations of the thermostat variables which clearly occur in ergodic systems may even be important in driving the system to fill phase space (the dynamical equations are, of course, coupled). This suggests thermostating p_η and, by analogy, the thermostat of p_η plus its thermostat, etc., to form a chain. Other methods of "shaking up" the system have also been suggested.[7–9,11]

The "new" dynamics, the Nosé–Hoover chain method, can be expressed as

$$\begin{aligned}
\dot{q}_i&=\frac{p_i}{m_i},\\
\dot{p}_i&=-\frac{\partial V(\mathbf{q})}{\partial q_i}-p_i\frac{p_{\eta_1}}{Q_1},\\
\dot{\eta}_i&=\frac{p_{\eta_i}}{Q_i},\\
\dot{p}_{\eta_1}&=\left[\sum_{i=1}^{N}\frac{p_i^2}{m_i}-NkT\right]-p_{\eta_1}\frac{p_{\eta_2}}{Q_2},\\
\dot{p}_{\eta_j}&=\left[\frac{p_{\eta_{j-1}}^2}{Q_{j-1}}-kT\right]-p_{\eta_j}\frac{p_{\eta_{j+1}}}{Q_{j+1}},\\
\dot{p}_{\eta_M}&=\left[\frac{p_{\eta_{M-1}}^2}{Q_{M-1}}-kT\right],
\end{aligned} \qquad (6)$$

where M thermostats have been included. The η's are again presented for completeness. These equations can be shown to have the phase space distribution

$$f(\mathbf{p},\mathbf{q},\mathbf{p}_\eta,\boldsymbol{\eta})\propto\exp\left\{-\frac{1}{kT}\left[V(\mathbf{q})+\sum_{i=1}^{N}\frac{p_i^2}{2m_i}+\sum_{i=1}^{M}\frac{p_{\eta_i}^2}{2Q_i}\right]\right\} \qquad (7)$$

and the conserved quantity

$$H'(\mathbf{p},\mathbf{q},\boldsymbol{\eta},\mathbf{p}_\eta)=V(\mathbf{q})+\sum_{i=1}^{N}\frac{p_i^2}{2m_i}+\sum_{i=1}^{M}\frac{p_{\eta_i}^2}{2Q_i}+NkT\eta_1+\sum_{i=2}^{M}kT\eta_i. \qquad (8)$$

Note that even in large systems, the addition of the extra thermostats is relatively inexpensive as they form a simple one dimensional chain. Only the first thermostat interacts with N particles.

A good choice for the thermostat masses will help the dynamics achieve the canonical distribution.[1–4] If very large masses are chosen, a distribution consistent with the microcanonical ensemble may result. If very small masses are chosen, the fluctuations of the momenta may be greatly inhibited. In Appendix B, a short argument is presented which suggest that the masses be taken to be $Q_1=NkT/\omega^2$ and $Q_j=kT/\omega^2$. This choice allows the thermostats to be in approximate resonance with both the system variables (the p's and q's), which are assumed to have fundamental frequency ω, and each other. As will be shown in the results section, the mass choice in the chain method is much less critical than in both the simple method[2] and some of the newer methods.[9]

The method presented above increases the size of the phase space and thus helps make the system ergodic. There are, however, several issues that must be examined. Consider a point in phase space $(\mathbf{q},\mathbf{p})$ with

$$\begin{aligned}
\frac{\partial V(\mathbf{q})}{\partial q_i}&=0,\\
p_i&=0.
\end{aligned} \qquad (9)$$

At such a point, the equations of motion for the Nosé–Hoover chain dynamics give $dq^n/dt^n=0$ for all n, which effectively stops the dynamics of the positions and momenta (Note this is equally true in Newtonian dynamics). We call such points Hoover holes, after Hoover who first began to look at the ergodicity of small systems in the modified dynamics. For the dynamics to be ergodic, the system must come infinitesimally close to the Hoover holes without actually visiting them. Therefore, the dynamics near the holes must be examined to be sure that the holes can reasonably be assumed to be of measure zero.

Hoover holes associated with specific values of the thermostat coordinates are fixed points of the entire Nosé–Hoover chain dynamics. If a fixed point is stable, then in its vicinity, the equations will have exponentially damped solutions which will drive the system into the point. This scenario is disastrous if an ergodic system is desired. The stability of a fixed point can be determined by examining the linearized equations motion about the point.[12,13] The

analysis proceeds by rewriting the Nosé–Hoover equations as the convenient first order system

$$\begin{aligned}
\dot{q}_i &= \frac{p_i}{m_i}, \\
\dot{p}_i &= -\frac{\partial V(\mathbf{q})}{\partial q_i} - p_i\zeta_1, \\
\dot{\zeta}_1 &= \frac{1}{Q_1}\left[\sum_{i=1}^{N}\frac{p_i^2}{m_i} - NkT\right] - \zeta_1\zeta_2, \\
\dot{\zeta}_j &= \frac{1}{Q_j}\left[Q_{j-1}\zeta_{j-1}^2 - kT\right] - \zeta_j\zeta_{j+1}, \\
\dot{\zeta}_M &= \frac{1}{Q_M}\left[Q_{M-1}\zeta_{M-1}^2 - kT\right],
\end{aligned} \tag{10}$$

where the variables $\zeta_j = \dot{\eta}_j$ have been introduced. The fixed point condition for the system is then given by the set of algebraic equations obtained from setting each of the time derivatives on the left side of Eqs. (11) equal to zero. This condition can be expressed as

$$\begin{aligned}
&\frac{\partial V(\mathbf{q})}{\partial q_i} = 0, \\
&p_i = 0, \\
&\zeta_1\zeta_2 + \alpha = 0, \\
&N\zeta_1^2 - \alpha - \zeta_2\zeta_3 = 0, \\
&\zeta_{j-1}^2 - \alpha - \zeta_j\zeta_{j+1} = 0, \\
&\zeta_{M-1}^2 - \alpha = 0,
\end{aligned} \tag{11}$$

where the mass choice, $Q_1 = NQ$ and $Q_j = Q$, has been introduced and $\alpha = kT/Q$. The linearized equations themselves are obtained by differentiating each quantity on the right side of Eq. (10) with respect to each variable in the system. The stability matrix, A, is defined by the quantities resulting from this differentiation evaluated at a fixed point [i.e., a solution of Eqs. (11)]. The eigenvalues of this matrix give the stability condition of the point. If the eigenvalues all have negative real parts, then the fixed point is purely stable. Now if the trace of a matrix is zero, the sum of the eigenvalues is zero. If the sum of the eigenvalues is zero, it can be concluded that either the eigenvalues are all zero or have both positive and negative real parts. Examination of Eqs. (10) and (11) and the linearized motion shows that the there are no solutions with all eigenvalues equal to zero, so we conclude that the latter must be true. A proof that the trace of A is zero is presented in Appendix C. Therefore, the fixed points of chain dynamics are not purely stable. It is also significant to note that the rate of change of the total phase space volume in the vicinity of the fixed point is related to the trace of the stability matrix by

$$\begin{aligned}
\sum_{i=1}^{N}\left(\frac{\partial \dot{p}_i}{\partial p_i} + \frac{\partial \dot{x}_i}{\partial x_i}\right) + \sum_{j=1}^{M}\frac{\partial \dot{\zeta}_j}{\partial \zeta_j} \\
= \sum_{i=1}^{N} A_{ii} + \sum_{j=1}^{M} A_{j+N,j+N} = \mathrm{Tr}(A).
\end{aligned} \tag{12}$$

Thus if the trace of A is zero, then Liouville's theorem (conservation of phase space volume) holds in the vicinity of the fixed points.[14] This implies that the fixed points are neither attractors or repellors.[12,15] These arguments only apply for $M > 1$, for $M = 1$ or the usual Nosé–Hoover dynamics there are no fixed points of the total dynamics. However, the rate of change of the total phase space volume is not everywhere zero, which suggests that the Nosé–Hoover chain dynamics does not have an underlying Hamiltonian structure. This fact could also be deduced from the stability conditions on the fixed points.[13] That is, the Nosé–Hoover dynamics admit spiral fixed points which are forbidden in Hamiltonian systems.

The preceding analysis cannot determine whether the system is ergodic. It does, however, give indications of when a system may not behave well in this respect. It is included for completeness and to indicate that Nosé–Hoover chain dynamics has some reasonable and desirable properties. A more useful analysis would involve showing that no periodic orbits exist in the dynamics, a periodic orbit stability analysis. This at present can only be done numerically. In the results section it will be shown that Nosé–Hoover chain dynamics fills phase space for some reasonable values of M.

The Lyapunov exponent gives a measure of the degree of chaos present in a dynamical system.[12,13,15,16] In general, the more chaotic the dynamics of a system, the more quickly it fills phase space. It is therefore important to study this quantity in chain dynamics. The calculation of Lyapunov exponents is based on dynamics cast in the generic form

$$\dot{\Gamma}(t) = F(\Gamma), \tag{13}$$

where $\Gamma(t)$ refers to a point in phase space [which for chain dynamics is $(\mathbf{q},\mathbf{p},\mathbf{p}_\eta)$]. In the first method used to calculated the exponents (Method I), two nearby trajectories are integrated for a small time interval τ, and the distance between them monitored. The initial separation is determined by

$$\Gamma'(0) = \Gamma(0) + \delta\Gamma(0), \tag{14}$$

where $\delta\Gamma(0)$ is a vector of norm ϵ. After an interval τ, the norm of $|\delta\Gamma(\tau)|$ is computed and saved. The vector $\delta\Gamma(\tau)$ is then renormalized to ϵ and the process repeated. The Lyapunov exponent is calculated from

$$\lambda = \frac{1}{N_\tau}\sum_{j=1}^{N}\log\left|\frac{\delta\Gamma_j(\tau)}{\epsilon}\right|. \tag{15}$$

In the second method (Method II), the linearized equations about the trajectory $\Gamma(t)$

$$\frac{d}{dt}\delta\Gamma(t) = M(t)\delta\Gamma(t), \tag{16}$$

$$\delta\Gamma(t) = T\exp\left[\int_0^t M(t')dt'\right]\delta\Gamma(0) \tag{17}$$

are solved as the trajectory $\Gamma(t)$ evolves. Here the matrix M is defined to be $M_{ij} = (\partial F_i/\partial\Gamma_j)|_{\Gamma=\Gamma(t)}$, and T is the time ordering operator. At time τ, $\delta\Gamma$ is renormalized and the process repeated. The exponent is calculated from the sum of the log of norms presented above in Eq. (15). In general, computing the exponent by these two methods serves as an excellent check on the results, however, it has been shown that Method I is consistently the more reliable.[16]

Assuming the dynamics produces the correct distribution, it is desirable to know how rapidly it samples the distribution. A measure of this is the rate of convergence of the time average of the potential and kinetic energy to their ensemble averages (the p's and q's are the variables of primary interest). Such a rate can be quantified by calculating the number of time steps necessary to obtain an error bar or error in the mean of desired tolerance. This number of time steps can then be compared to the number of Monte Carlo steps needed to give the same error bar where the Monte Carlo calculation is performed by directly sampling the distribution of interest (i.e., the perfect stochastic calculation). An efficiency can be calculated which is the ratio of the number of time steps to the number of Monte Carlo steps $R = S_{\rm MD}/S_{\rm MC}$. Thus the larger is R, the less efficient the method where R has a lower limit of 1. The error bars for the time averages are calculated using the block averaging technique[17] which takes into account correlations which may exist in the data. The Monte Carlo data is uncorrelated by definition. The error bar of the average or error in the mean is then given analytically as the standard deviation of the quantity (averaged over the distribution) divided by the square root of the number of steps. The efficiency obviously depends on the method of integration and the time step chosen to perform the dynamics but does give a useful measure convergence. Two values of the efficiency are calculated, R_q, which measures the convergence of the average potential energy and R_p, which measures the convergence of the average kinetic energy.

The velocity Verlet integrator[18] is used to integrate the Nosé–Hoover chain equations. The position equations are deterministic and the velocity equations are solved iteratively to a convergence level of 10^{-14}. The model problems studied in the next section were integrated with time steps of Δt=0.016, Δt=0.005, Δt=0.0016, and Δt=0.0005 for systems using $Q_i = 10$, $Q_i = 1$, $Q_i = 0.1$, and $Q_i = 0.01$, respectively. These choices give energy (H') conservation to a few parts in 10^5. {For reference, integrating the harmonic oscillator [m=1,ω=1,$q(0)$=1,$v(0)$=1], to the same tolerance requires a time step of 0.016.} A great advantage of the chain method is that there is little or no degradation in energy conservation upon the addition of thermstats beyond M=1. All runs were 1.5×10^6 time steps. In the calculation of the Lyapunov exponents, we compared the exponent for choices of τ ranging from $10\Delta t$ to $100\Delta t$, and found good agreement between Methods I and II in this range.

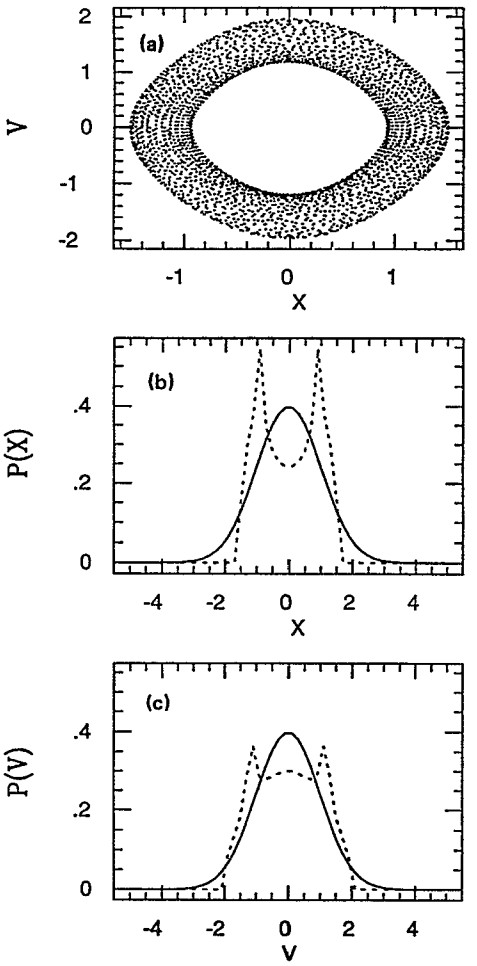

FIG. 1. (a) Density plot of the Nosé–Hoover dynamics of a harmonic oscillator [$q(0) = 1, p(0) = 1, p_\eta(0) = 1, Q = 1$]. (b) Position distribution function obtained from Nosé–Hoover dynamics of a harmonic oscillator (dotted line). The solid line is the exact result. (c) Velocity distribution function obtained from Nosé–Hoover dynamics of a harmonic oscillator (dotted line). The solid line is the exact result.

III. RESULTS

Two systems were chosen to illustrate the new method. The first, is a one dimensional harmonic oscillator ($m = 1, \omega = 1, Q_i = 1$) with initial condition [$q(0) = 0, p(0) = 1, p_{\eta_i}(0) = 1$] and kT=1. In Fig. 1, a density map and the projected distribution functions are presented for the usual Nosé–Hoover dynamics (M=1). The dynamics does not fill space. Also, if the initial conditions are changed, ($q = 0, p = 1, p_\eta = 10$), the results are changed (see Fig. 2). This is unacceptable as an invariant probability distribution is desired. Similar results have been found by others.[2,7] The Nosé–Hoover chain dynamics, (M=2), gives rather different results (see Fig. 3). The distribution functions seem to be good approximations to the canonical results and the dynamics fills space. Changes in the initial conditions did not have an appreciable effect on the results.

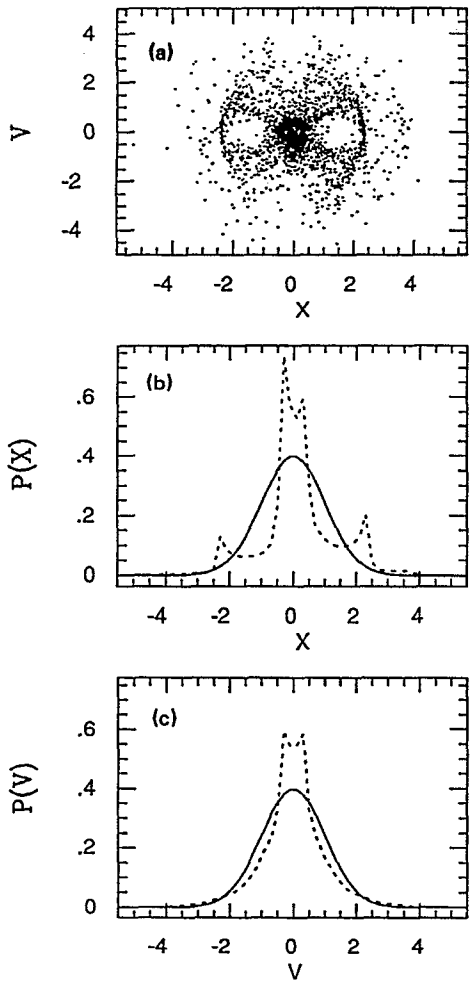

FIG. 2.(a) Density plot of the Nosé–Hoover dynamics of a harmonic oscillator [$q(0) = 1, p(0) = 1, p_\eta(0) = 10, Q = 1$]. (b) Position distribution function obtained from Nosé–Hoover dynamics of a harmonic oscillator (dotted line). The solid line is the exact result. (c) Velocity distribution function obtained from Nosé–Hoover dynamics of a harmonic oscillator (dotted line). The solid line is the exact result.

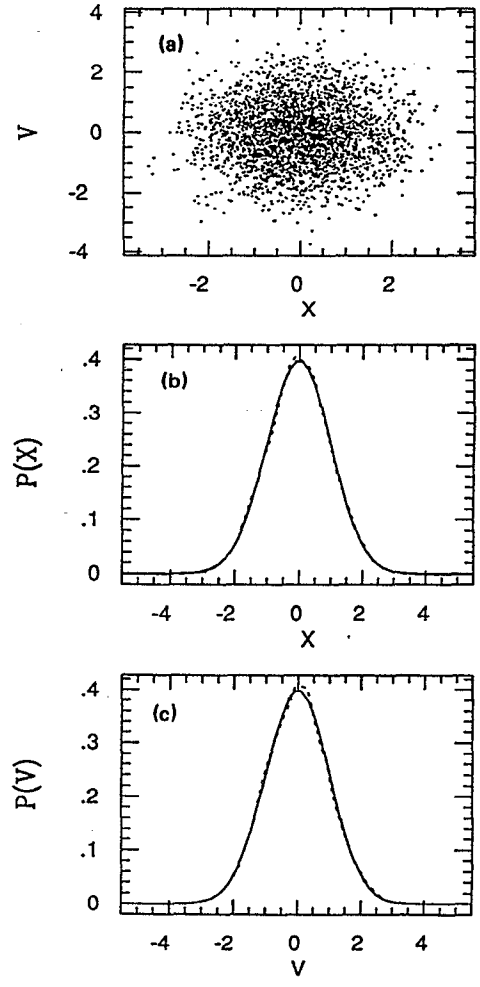

FIG. 3.(a) Density plot of the Nosé–Hoover chain dynamics ($M=2, Q=1$) of a harmonic oscillator [$q(0) = 1, p(0) = 1, p_\eta(0) = 1$]. (b) Position distribution function obtained from Nosé–Hoover dynamics of a harmonic oscillator (dotted line). The solid line is the exact result. (c) Velocity distribution function obtained from Nosé–Hoover dynamics of a harmonic oscillator (dotted line). The solid line is the exact result.

In addition, the choice of thermostat mass is not critical in this method unlike both the original[2] and some of the newer methods.[9] Rather, for all the values attempted, $Q=100$, $M=5$, $Q=10$, $M=2$, $Q=0.1$, $M=2$, and $Q=0.01$, $M=2$, the canonical distribution was generated.

The Lyapunov exponents for systems containing $M=1$–15 thermostats were calculated for wide variety of initial conditions ($Q=1$). The two methods used to obtain the exponents (see Methods) were found to be in good agreement as is shown in Tables I and II. In Fig. 4, the exponents are plotted as a function of M. The exponents become increasing large with M and around $M=4,5$ become competitive with those determined by Kusnezov *et al.* for their method.[7] However, the Lyapunov exponents include information about the dynamics of thermostat variables which are not of primary interest. In Table III, the efficiency of chain dynamics in the convergence of the average potential and kinetic energy is calculated for a variety of parameters (see Sec. II). The results indicate that the parameter set $Q=1, M=5$ converges most rapidly. For this set, the chain method is found to be competitive with the method of Kusnezov *et al.* ($Q_p = 1, Q_q = 1$) for the convergence of the potential energy (see Table III). The average kinetic energy converges very rapidly in the latter

TABLE I. Comparison between Methods I and II of the convergence of the Lyapunov exponent for $M=4$, and $\tau=10\Delta t$.

Steps	λ(Method I)	λ(Method II)
100	0.2983	0.2954
1 000	0.2517	0.2516
2 000	0.2659	0.2660
3 000	0.2290	0.2293
4 000	0.2196	0.2200
5 000	0.2371	0.2370
6 000	0.2465	0.2460
7 000	0.2391	0.2392
8 000	0.2381	0.2382
9 000	0.2402	0.2402
10 000	0.2385	0.2384

TABLE II. Comparison between Methods I and II of the convergence of the Lyapunov exponent for $M=6$, and $\tau=10\Delta t$.

Steps	λ(Method I)	λ(Method II)
100	0.4608	0.4571
1 000	0.4366	0.4368
2 000	0.3829	0.3832
3 000	0.3359	0.3356
4 000	0.3273	0.3268
5 000	0.3139	0.3129
6 000	0.2939	0.2936
7 000	0.3025	0.3028
8 000	0.2966	0.2968
9 000	0.2997	0.2998
10 000	0.2890	0.2897

method which may be due to the use of the third power of the momentum thermostat in the coupling term (see Appendix A). The calculated efficiency is a subjective measure that depends on the method of integration and the time step used.

For a harmonic oscillator, the Hoover holes do not have a pathological effect. The phase space in a harmonic oscillator is such that $p=0$ can be visited when $q\neq 0$ and vice versa, which reduces the effect of the hole particularly on the integrated distributions [$P(v)$ and $P(q)$]. To complete the analysis, pairs of trajectories within a radius of 10^{-8} about the hole were examined. Lypaonov exponents similar to those reported in Fig. 4 for a given value of M were obtained ($Q=1$). The fact that a positive exponent is obtained implies that the holes are not attractive and seem to be of zero measure, consistent with the analysis in Sec. II.[15]

The second system studied is a one dimensional free particle ($Q=1$). The Nosé–Hoover chain dynamics can only give canonically distributed velocity on the half space

TABLE III. Efficiency of chain dynamics for the harmonic oscillator.[a]

Q	M	R_q	R_p
1.0	2	230	230
1.0	5	230	110
1.0	15	230	110
10.0	5	370	370
0.1	5	730	70
0.01	5	2300	150

[a]For the method of Kusnezov *et al.* ($Q_p=1, Q_q=1$), $R_q=230$ and $R_p=3$.

$v\geqslant 0$. When $v=0$, the dynamics stops for all times [$d^n q(t)/dt^n=0$ for all n]. The dynamics was never found to stop, but neither could it pass through the Hoover hole. (The holes seem to be of measure zero and are not attractive.) The dynamics is symmetric about the hole since the equations of motion do not depend on the sign of v. Thus an identical trajectory can be generated on the other half of phase space with no cost. In Fig. 5, the velocity distribution of the free particle is presented for $M=1,2,3$. The canonical distribution is recovered when $M=3$. As discussed in Appendix A, the functions chosen by Kusnezov *et al.* for use in their method are not appropriate for this system.

IV. DISCUSSION

The idea of thermostating the extended variable is potentially quite powerful. In stiff complex systems such as proteins, it is difficult to start near equilibrium. In such cases, large unphysical oscillations in the temperature may develop. It is expected that additional thermostats will effectively damp such oscillations. Similarly, oscillations can develop in the volume in constant pressure–constant tem-

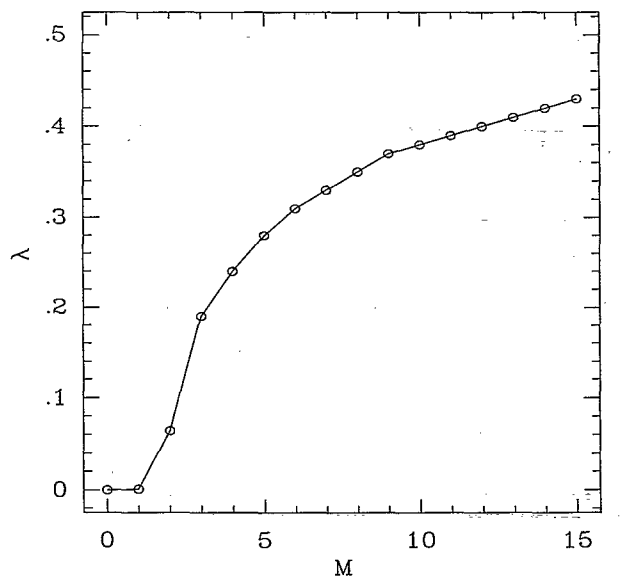

FIG. 4. Lyapunov exponent for the chain dynamics of a harmonic oscillator as a function of the number of thermostats, M ($Q=1$).

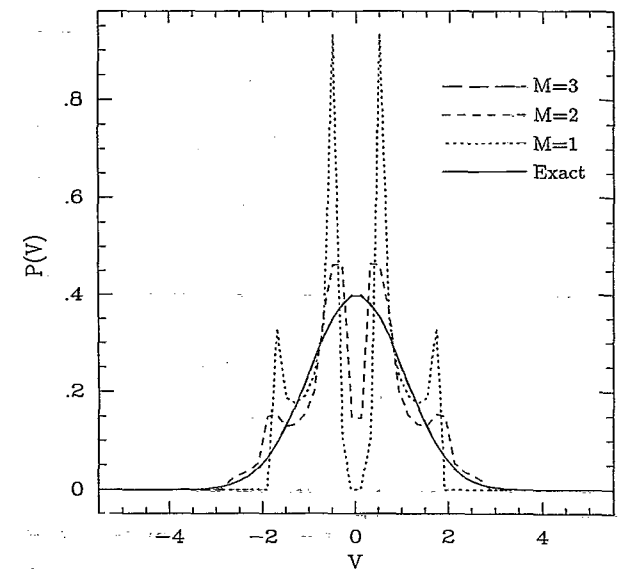

FIG. 5. Velocity distribution function obtained from Nosé–Hoover chain dynamics ($M=1,2,3, Q=1$) of a free particle. The solid line is the exact result.

perature simulations. As the momentum of the extended variable that drives volume is distributed canonically, it can also be thermostated (the proof goes through straightforwardly). Again, this should help damp the unphysical oscillations resulting in more stable simulations.

In summary, a modification of Nosé–Hoover dynamics which we call Nosé–Hoover chain dynamics has been shown to give a very good approximation to the canonical ensemble even in pathological cases. The idea of thermostating extended variables will likely find wide application.

ACKNOWLEDGMENTS

The research described herein was supported by the National Science Foundation under Grant No. CHE-8722481. One of us (G.M.) would like to acknowledge an NSF Posdoctoral Research Associateship in Computational Science and Engineering (ASC-91-08812). In addition, we would like to thank Bruce Berne for many insights incorporated into this paper. We would also like to thank Professor P. Pechukas and Professor L. Schulman for useful discussions on chaos theory, and Professor W. Hoover, Professor S. Nosé, and Dr. J. Jellinek for commenting on the paper before publication.

APPENDIX A

The Nosé–Hoover equations are in fact a subset of the more general set of equations,[1,7]

$$\begin{aligned}
\dot{q}_i &= \frac{p_i}{m_i} - h_q(\eta_q) F_q(p_i,q_i), \\
\dot{p}_i &= -\frac{\partial V(\mathbf{q})}{\partial q_i} - h_p(\eta_p) F_p(p_i,q_i), \\
\dot{\eta}_p &= \frac{1}{Q_p}\left[\sum_{i=1}^{N} \frac{p_i}{m_i} F_p(p_i,q_i) - T\frac{\partial F_p(p_i,q_i)}{\partial p_i}\right], \\
\dot{\eta}_q &= \frac{1}{Q_q}\left[\sum_{i=1}^{N} \frac{\partial V(\mathbf{q})}{\partial q_i} F_q(p_i,q_i) - kT\frac{\partial F_q(p_i,q_i)}{\partial q_i}\right],
\end{aligned} \tag{A1}$$

where F_q, G_q, h_q, h_p are arbitrary functions. These equations have the conserved quantity

$$\begin{aligned}
H' = {} & H(p,q) + Q_p g_p(\eta_p) + Q_q g_q(\eta_q) \\
& + kT \int_0^t \left[h_q(\eta_q) \sum_{i=1}^{N} \frac{\partial F_q(p_i,q_i)}{\partial q_i} \right. \\
& \left. + h_p(\eta_p) \sum_{i=1}^{N} \frac{\partial F_p(p_i,q_i)}{\partial p_i} \right],
\end{aligned} \tag{A2}$$

where $h_l = dg_l/d\eta_l$. This is a powerful generalization that can be used to generated canonical dynamics for variety systems (i.e., Lie algebras[3,7]). The Nosé–Hoover equations are generated from the specific choice $F_q = h_q = 0$ and $g_p = \eta_p^2/2$, $h_p = \eta$, $F_p = p$. Such a choice is more general than it may first appear as can seen by examining the position dependence of the functions F_q and F_p. This dependence must be consistent with the boundary condition of a given problem. Therefore, a general purpose method must take these functions to be independent of position. Furthermore, the proof that the dynamical system, Eq. (1), gives rise to the canonical distribution relies on the identities,[3,7]

$$\begin{aligned}
kT\left\langle \frac{\partial F_q(p_i,q_i)}{\partial q_i} \right\rangle &= \left\langle F_q(p_i,q_i) \frac{\partial H(\mathbf{p},\mathbf{q})}{\partial q_i} \right\rangle, \\
kT\left\langle \frac{\partial F_p(p_i,q_i)}{\partial p_i} \right\rangle &= \left\langle F_p(p_i,q_i) \frac{\partial H(\mathbf{p},\mathbf{q})}{\partial p_i} \right\rangle,
\end{aligned} \tag{A3}$$

where the average is, itself, over the canonical distribution. If the F's are independent of position, F_q must be taken to be zero. This argument leads naturally to a Nosé–Hoover form if the dependence of $G_p(p)$ and $h_p(\eta_p)$ is chosen to be linear, i.e., the simplest nontrivial choice. Chain dynamics maintains this form. It is, however, possible to derive a general set of equations from which chain dynamics emerges as a specific choice of functions.

In studying simple bound problems, Kusnezov *et al.* have advocated the choice, $F_q = q^3$, $F_p = p$, $h_q = \eta_q$, $h_p = \eta_p^3$.[7] With these choices the trace of the stability matrix is zero which guarantees certain properties of the dynamics in the vicinity of the fixed points (see Sec. II). The stability matrix of chain dynamics also has a zero trace (see Appendix C). In addition, the fixed points of chain dynamics occur at their natural places $[p_i = 0, \partial V(\mathbf{q})/\partial q_i = 0]$ while fixed points of the more complex method do not.

The equations of motion [Eq. (1)] with the choice of functions of Kusnezov *et al.* are rather stiff. For a harmonic oscillator ($m=1, \omega=1, kT=1$) integration by velocity Verlet did not conserve H' well. In the spirit of the iterative scheme used to integrate the Nosé–Hoover chains, the set of first order differentials in Eq. (1) were integrated by iterating the general form

$$b(t) = b(0) + [\dot{b}(0) + \dot{b}(t)]\frac{dt}{2} \tag{A4}$$

to convergence. A time step of 0.001 was needed to obtain reasonable H' conservation for the oscillator. About five iterations were needed for convergence.

The dynamics proposed by Winkler[9] can be expressed as

$$\begin{aligned}
\dot{q}_i &= \frac{p_i}{m_i}, \\
\dot{p}_i &= -\frac{\partial V(\mathbf{q})}{\partial q_i} + \frac{2p_\eta}{\eta} p_i, \\
\dot{\eta} &= \frac{p_\eta}{Q}, \\
\dot{p}_\eta &= -\frac{2}{\eta}\left[\sum_{i=1}^{N} \frac{p_i^2}{m_i} - (N-\tfrac{1}{2})kT\right].
\end{aligned} \tag{A5}$$

This can be shown to have the distribution function

$$f(\mathbf{p},\mathbf{q},p_\eta,\eta) \propto \frac{1}{\eta}\exp\left\{-\frac{1}{kT}\left[V(\mathbf{q}) + \sum_{i=1}^{N}\frac{p_i^2}{2m_i} + \frac{p_\eta^2}{2Q}\right]\right\} \tag{A6}$$

with conserved quantity

$$H' = H(p,q) + \frac{p_\eta^2}{2Q} - (2N-1)kT \log \eta. \tag{A7}$$

The variable η appears explicitly in the dynamical equations but has an "unbounded" probability distribution. Therefore, the dynamical equations appear to be rather poorly behaved in some regions of phase space, particularly when η is small. These regions are not sampled by the dynamics as the conserved quantity restricts phase space such that $\eta = \exp\{[H(p,q) + p_\eta^2/2Q - E]/(2N-1)kT\}$. As E is a constant and $H(p,q)$ and p_η have bounds (their distribution functions decay exponentially), η is "bounded."{The inverse of η is bounded from above by $\exp[(E - V_{\min})/(2N-1)kT]$, where $V_{\min}$ is the global minimum of the potential energy surface.} However, if another thermostat is added to the dynamics, either to control η or some subset of the degrees of freedom in the system then the restriction imposed by the conserved quantity is insufficient "to bound" the thermostat positions and avoid regions of phase space that are (numerically) unstable for the dynamics. In fact, the instability was first noticed in attempts to numerically integrate a chainlike ansatz within this formalism. The method is therefore not as useful or flexible as the usual Nosé–Hoover construction. Note that though there is another form of the Winkler method with slightly different equations of motion, it has the same difficulties as the more natural variant discussed above.

APPENDIX B

In order to determine reasonable values for the thermostat masses, a second order equation of motion is generated for each of the $\dot\eta_j$ from the time derivative of $\ddot\eta_j$

$$\frac{d^2\dot\eta_1}{dt^2} = \left\{\frac{2}{Q_1}\left[\sum_{i=1}^{N}\frac{\partial V(\mathbf{q})}{q_i}\frac{p_i}{m_i}\right] - \frac{\dot\eta_2}{Q_1}\left[\sum_{i=1}^{N}\frac{p_i^2}{m_i} - NkT\right]\right\} - \dot\eta_1\left\{\sum_{i=1}^{N}\frac{p_i^2}{m_i} - \dot\eta_2^2 + \dot\eta_2\dot\eta_3 + \frac{1}{Q_2}[Q_1\dot\eta_1^2 - kT]\right\},$$

$$\frac{d^2\dot\eta_2}{dt^2} = \left\{\frac{2\dot\eta_1}{Q_2}\left[\sum_{i=1}^{N}\frac{p_i^2}{m_i} - NkT\right] - \frac{\dot\eta_3}{Q_2}[Q_1\dot\eta_1^2 - kT]\right\} - \dot\eta_2\left\{\frac{2\dot\eta_1^2 Q_1}{Q_2} - \dot\eta_3^2 + \frac{1}{Q_3}[Q_2\dot\eta_2^2 - kT] - \dot\eta_3\dot\eta_4\right\},$$

$$\frac{d^2\dot\eta_j}{dt^2} = \left\{\frac{2\dot\eta_{j-1}}{Q_{j-1}}[Q_{j-2}\dot\eta_{j-2}^2 - kT] - \frac{\dot\eta_{j+1}}{Q_j}[Q_{j-1}\dot\eta_{j-1}^2 - kT]\right\} - \dot\eta_j\left\{\frac{2\dot\eta_{j-1}^2 Q_{j-1}}{Q_j} - \dot\eta_{j+1}^2 + \frac{1}{Q_{j+1}}[Q_j\dot\eta_j^2 - kT] - \dot\eta_{j+1}\dot\eta_{j+2}\right\}, \tag{B1}$$

$$\frac{d^2\dot\eta_{M-1}}{dt^2} = \left\{\frac{2\dot\eta_{M-2}}{Q_{M-1}}[Q_{M-3}\dot\eta_{M-3}^2 - kT] - \frac{\dot\eta_M}{Q_{M-1}}[Q_{M-2}\dot\eta_{M-2}^2 - kT]\right\} - \dot\eta_{M-1} \times\left\{\frac{2\dot\eta_{M-2}^2 Q_{M-2}}{Q_{M-1}} - \dot\eta_M^2 + \frac{1}{Q_M}[Q_{M-1}\dot\eta_{M-1}^2 - kT]\right\},$$

$$\frac{d^2\dot\eta_M}{dt^2} = \left\{\frac{2\dot\eta_{M-1}}{Q_M}[Q_{M-2}\dot\eta_{M-2}^2 - kT]\right\} - \dot\eta_M\left\{\frac{2\dot\eta_{M-1}^2 Q_{M-1}}{Q_M}\right\}.$$

These equations can be solved *individually*, in the limit η_i is fast compared to η_{i-1} and η_{i+1}, while η_{i+2} moves on the same time scale. This permits us to take functions of η_{i-1} and η_{i+1} equal to their average values.[3] The result is

$$\frac{d^2\dot\eta_1}{dt^2} = -\dot\eta_1\left[\frac{2NkT}{Q_1} - \frac{2kT}{Q_2}\right] - \frac{Q_1}{Q_2}\dot\eta_1^3,$$

$$\frac{d^2\dot\eta_j}{dt^2} = -\dot\eta_j\left[\frac{2kT}{Q_j} - \frac{2kT}{Q_{j+1}}\right] - \frac{Q_{j-1}}{Q_{j+1}}\dot\eta_j^3, \tag{B2}$$

$$\frac{d^2\dot\eta_M}{dt^2} = -\dot\eta_M\left[\frac{2kT}{Q_M}\right].$$

The choices $Q_1 = NkT/\omega^2$ and $Q_j = kT/\omega^2$ give thermostats 1 to $M-1$ an average "frequency" of ω. This frequency is calculated by averaging the $\dot\eta_i^2$ in the third order term over the distribution function. The Mth thermostat oscillates with frequency 2ω. The arbitrary parameter ω is chosen based on the properties of potential energy surface (phonon frequencies, etc). Several approximations have gone into the analysis and, in fact, the choice of mass itself violates some of the approximations. This is only meant to give a rough estimate.

APPENDIX C

In this Appendix, a proof that the trace of the stability matrix is zero for chain dynamics is presented. The diagonal elements of A, the stability matrix, are

$$A_{ii} = -\zeta_1, \quad i=1,N,$$

$$A_{(N+j)(N+j)} = -\zeta_j, \quad j=1,M, \tag{C1}$$

where the ζ's evaluated at a fixed point. The trace of A is then

$$-\mathrm{Tr}(A) = N\zeta_1 + \sum_{j=2}^{M}\zeta_j. \tag{C2}$$

From the fixed point equations, Eqs. (11), it is immediately clear that $\zeta_{M-1} = \pm\sqrt{\alpha}$. Solving for ζ_M in terms of ζ_{M-2} in Eqs. (11) and substituting into the trace gives

$$-\mathrm{Tr}(A) = N\zeta_1 + \sum_{j=2}^{M-2}\zeta_j + \sqrt{\alpha} + \frac{1}{\sqrt{\alpha}}(\zeta_{M-2}^2 - \alpha) = N\zeta_1 + \sum_{j=2}^{M-2}\zeta_j + \frac{1}{\sqrt{\alpha}}\zeta_{M-2}^2. \tag{C3}$$

Similarly, solving for ζ_{M-2} in terms of ζ_{M-3}, substituting into the trace and simplifying gives

$$-\mathrm{Tr}(A)=N\zeta_1+\sum_{j=2}^{M-3}\zeta_j-\frac{1}{\sqrt{\alpha}}\zeta_{M-3}^2+\frac{1}{\alpha\sqrt{\alpha}}\zeta_{M-3}^4. \tag{C4}$$

At this point, the other end of the equation is simplified. The variable $N\zeta_1$ is replaced by $N\zeta_1=(\alpha+\zeta_2\zeta_3)/\zeta_1$ and ζ_2 is replaced by $\zeta_2=-\alpha/\zeta_1$. Substituting into the trace and simplifying gives

$$-\mathrm{Tr}(A)=-\frac{1}{\alpha}\zeta_2^2\zeta_3+\sum_{j=3}^{M-3}\zeta_j-\frac{1}{\sqrt{\alpha}}\zeta_{M-3}^2+\frac{1}{\alpha\sqrt{\alpha}}\zeta_{M-3}^4. \tag{C5}$$

Now, substituting $\zeta_2^2=\alpha+\zeta_3\zeta_4$ and simplifying gives

$$-\mathrm{Tr}(A)=-\frac{1}{\alpha}\zeta_3^2\zeta_4+\sum_{j=4}^{M-3}\zeta_j-\frac{1}{\sqrt{\alpha}}\zeta_{M-3}^2+\frac{1}{\alpha\sqrt{\alpha}}\zeta_{M-3}^4. \tag{C6}$$

Similarly, substituting $\zeta_3^2=\alpha+\zeta_4\zeta_5$ and simplifying gives

$$-\mathrm{Tr}(A)=-\frac{1}{\alpha}\zeta_4^2\zeta_5+\sum_{j=5}^{M-3}\zeta_j-\frac{1}{\sqrt{\alpha}}\zeta_{M-3}^2+\frac{1}{\alpha\sqrt{\alpha}}\zeta_{M-3}^4. \tag{C7}$$

Each subsequent substitution cancels the next term in the sum until we get to $M-4$, where

$$-\mathrm{Tr}(A)=-\frac{1}{\alpha}\zeta_{M-4}^2\zeta_{M-3}+\zeta_{M-3}-\frac{1}{\sqrt{\alpha}}\zeta_{M-3}^2+\frac{1}{\alpha\sqrt{\alpha}}\zeta_{M-3}^4. \tag{C8}$$

Inserting the usual term $\zeta_{M-4}=\alpha+\zeta_{M-3}\zeta_{M-2}$ gives

$$-\mathrm{Tr}(A)=-\frac{1}{\alpha}\zeta_{M-3}^2\zeta_{M-2}-\frac{1}{\sqrt{\alpha}}\zeta_{M-3}^2+\frac{1}{\alpha\sqrt{\alpha}}\zeta_{M-3}^4. \tag{C9}$$

Finally, using the fact that $\zeta_{M-2}=(\zeta_{M-3}-\alpha)/\sqrt{\alpha}$ gives

$$-\mathrm{Tr}(A)=-\frac{1}{\alpha\sqrt{\alpha}}\zeta_{M-3}^2(\zeta_{M-3}^2-\alpha)-\frac{1}{\sqrt{\alpha}}\zeta_{M-3}^2+\frac{1}{\alpha\sqrt{\alpha}}\zeta_{M-3}^4=0, \tag{C10}$$

which completes the proof.

The zero trace condition can also be used to show that Louiville's theorem holds in the vicinity of the fixed points. In this region, the linearized equations hold

$$\dot{x}_i=\sum_j A_{ij}x_j, \tag{C11}$$

where the x are a general set of variables (i.e., x represents the p's, q's, and ζ's). Now according to Liouville's theorem, the condition for incompressible phase space volume is

$$\sum_{i=1}^{N}\frac{\partial\dot{x}_i}{\partial x_i}=0. \tag{C12}$$

Now differentiating $\dot{x}_i$ with respect to x_i gives

$$\sum_{i=1}^{N}A_{ii}=0, \tag{C13}$$

which is equal to zero if the matrix, A is traceless. Thus the phase space volume is conserved in the region of validity of the equations and the fixed points are neither attractors nor repellors.

[1] S. Nosé, J. Chem. Phys. **81**, 511 (1984).
[2] W. G. Hoover, Phys. Rev. A **31**, 1695 (1985).
[3] S. Nosé, Prog. Theor. Phys. Supp. **103**, 1 (1991).
[4] W. G. Hoover, *Computational Statistical Mechanics* (Elsenieer, New York, 1991).
[5] S. Toxvaerd and O. H. Olson, Ber. Bunsenges. Phys. Chem. **94**, 274 (1990).
[6] H. C. Andersen, J. Chem. Phys. **72**, 2384 (1980).
[7] D. Kusnezov, A. Bulgac, and W. Bauer, Ann. Phys. **204**, 155 (1990).
[8] I. P. Hamilton, Phys. Rev. A **42**, 7467 (1990).
[9] R. G. Winkler, Phys. Rev. A **45**, 2250 (1992).
[10] J. Jellinek and R. S. Berry, Phys. Rev. A **40**, 2816 (1989).
[11] J. Jellinek, J. Phys. Chem. **92**, 3163 (1988).
[12] A. J. Lichtenberg and M. A. Lieberman, *Regular and Stochastic Motion* (Springer, New York, 1983).
[13] Michael Tabor, *Chaos and Integrability in Nonlinear Dynamics* (Wiley, New York, 1989).
[14] V. I. Arnold, *Mathematical Methods of Classical Mechanics* (Springer, New York, 1978).
[15] David Ruelle, *Chaotic Evolution and Strange Attractors* (Cambridge University, New York, 1983).
[16] A. Wolf, in *Chaos*, edited by Arun V. Holden (Princeton University, Princeton, 1986).
[17] J. Cao and B. J. Berne, J. Chem. Phys. **91**, 6359 (1989).
[18] W. C. Swope, H. C. Andersen, P. H. Berens, and K. R. Wilson, J. Chem. Phys. **76**, 637 (1982).